JTTEE5 16:349–354
DOI: 10.1007/s11666-007-9029-4
1059-9630/$19.00 © ASM International

Technical Note

Hot Corrosion Behavior of HVOF Sprayed Coatings on ASTM SA213-T11 Steel

H.S. Sidhu, B.S. Sidhu, and S. Prakash

(Submitted September 16, 2006; in revised form December 22, 2006)

Cr_3C_2-NiCr, NiCr, WC-Co and Stellite-6 alloy coatings were sprayed on ASTM SA213-T11 steel using the HVOF process. Liquid petroleum gas was used as the fuel gas. Hot corrosion studies were conducted on the uncoated as well as HVOF sprayed specimens after exposure to molten salt at 900 °C under cyclic conditions. The thermo-gravimetric technique was used to establish the kinetics of corrosion. XRD, SEM/EDAX and EPMA techniques were used to analyze the corrosion products. All these overlay coatings showed a better resistance to hot corrosion as compared to that of uncoated steel. NiCr Coating was found to be most protective followed by the Cr_3C_2-NiCr coating. WC-Co coating was least effective to protect the substrate steel. It is concluded that the formation of Cr_2O_3, NiO, $NiCr_2O_4$, and CoO in the coatings may contribute to the development of a better hot-corrosion resistance. The uncoated steel suffered corrosion in the form of intense spalling and peeling of the scale, which may be due to the formation of unprotective Fe_2O_3 oxide scale.

Keywords coating-substrate interaction, corrosion of HVOF coatings, HVOF coatings

1. Introduction

Metals and alloys sometimes experienced accelerated oxidation when their surfaces are covered by a thin film of fused salt in an oxidizing atmosphere at elevated temperatures. This mode of attack is called ''hot corrosion,'' where a porous non-protective oxide scale is formed at the surface and sulfides in the substrate (Ref 1). When considering coal-gasification processes, metallic components are exposed to severe corrosion atmospheres and high-temperatures. The corrosive nature of the gaseous environments (i.e. environments containing O, S, C, and small amount of V) may cause rapid material degradation and result in the premature failure of components (Ref 2). Boiler steels are unable to simultaneously meet the requirements for both the high-temperature strength and the high-temperature corrosion resistance, so protective coatings are used to counter the latter (Ref 3). Metallic coatings sprayed on super-heater tubes have reduced the erosion and corrosion in selected cases (Ref 4).

The high velocity oxy fuel (HVOF) process is reported to be a versatile technology and has been adopted by many industries due to its flexibility, cost effectiveness and the superior quality of coating produced (Ref 5). The objective of the present work is to characterize the high-temperature corrosion mechanisms for HVOF alloy coatings on boiler steel namely ASTM SA213-T11 in an aggressive environment of molten salt (Na_2SO_4-60%V_2O_5). X-ray diffraction (XRD), scanning electron microscopy/energy-dispersive analysis (SEM/EDAX) and electron probe microanalysis (EPMA) techniques have been used to characterize corrosion products after hot corrosion under cyclic conditions at 900 °C.

H.S. Sidhu, Department of Mechanical Engineering, Yadavindra College of Engineering, Talwandi Sabo, Bathinda, Punjab, India; **B.S. Sidhu,** Department of Mechanical Engineering, G.Z.S. College of Engineering and Technology, Bathinda, Punjab, India; and **S. Prakash,** Department of Metallurgical and Materials Engineering, Indian Institute of Technology, Roorkee, Uttaranchal, India. Contact e-mail: mjsidhu@rediffmail.com.

2. Experimental Procedure

The boiler tube steel, ASTM SA213-T11, have been used as substrate. The chemical composition of the substrate steel is given in Table 1. This material is used as boiler-tube material in some power plants in northern India. The dimensions of the steel samples were 3×15 15 mm^3. The specimens were polished and grit-blasted with Al_2O_3 (grit 45) prior to application of the HVOF spray coatings. The details of the alloys powders, used in the study are given in Table 2. The first three alloys, i.e., Cr_3C_2-NiCr, WC-12Co and Stellite-6 are in powder form and the forth alloy, i.e., Ni-20Cr is in wire form, having a diameter of 3.17 mm. The powders and wire are commercially available and supplied by M/S Metallizing Equipment Co., Jodhpur, Rajasthan (India).

Around 300 μm thick coatings were deposited by Metallizing Equipment Co., Jodhpur, Rajasthan (India) with a commercial HIPOJET-2100 and HIJET-9600 apparatus operating with oxygen and liquid petroleum gas (LPG) as the fuel gases. The steel substrates were cooled with compressed air jets during and after spraying. The spraying parameters are given in Table 3**.** The coatings have been characterized prior to perform the present hot

Table 1 Chemical composition (wt.%) of ASTM SA213-T11 boiler tube steels

C	Mn	Si	S	P	Cr	Mo	Fe
0.15	0.3-0.6	0.5-1	0.03	0.03	1-1.5	0.44-0.65	Balance

Table 2 Chemical composition and particle size of alloys

Powder Name	Chemical composition, wt.%	Particle size
Cr_3C_2-NiCr	75Cr_3C_2, 20Ni, 5Cr	−45 + 15 μm
WC-Co	88WC-12Co	−45 + 15 μm
Stellite-6	28Cr,4.9W,1.2C,2.3Ni, 1.1Si,2.7Fe,BalCo.	−45 + 15 μm
NiCr (Wire)	80Ni-20Cr	Diameter of 3.17 mm

Table 3 Spray parameters employed during HVOF spraying

	Hijet-9600 (Wire)	Hipojet-2100 (Powder)
Oxygen flow rate	250 LPM	250 LPM
Fuel (LPG) flow rate	60 LPM	70 LPM
Air flow rate	900 LPM	6200 LPM
Spray distance	0.2 m	0.2 m
Wire/Powder feed rate	0.0013 kg/s	0.005 kg/s

corrosion studies, and the results have been published elsewhere (Ref 6). Porosity measurements have been made after polishing the specimens. Image analyzer having software Dewinter Material Plus 1.01 based on ASTM B276 was utilized to determine the porosity values. Images of the surface of the specimens were obtained through an attached PMP3 Inverted Metallurgical Microscope made in Japan. The NiCr wire coating shows the least value of porosity (>1%) comparable to the other coatings.

2.1 Corrosion Tests

Cyclic oxidation studies were performed in molten salt (Na_2SO_4-60% V_2O_5) for 50 cycles, with each cycle consisting of a 1-h heating period at 900 °C, followed by 20 min cooling at room temperature. The aim of the cyclic loading is to create severe testing conditions. The studies were performed on uncoated and coated samples for the comparison of the results.

The uncoated sample was mirror-polished, down to 1 μm by alumina wheel-cloth polishing before performing the corrosion studies. The coated samples were also subjected to wheel cloth polishing for 10 min before corrosion tests. A Na_2SO_4-60% V_2O_5 coating of uniform thickness of 3-5 mg/cm^2 was applied with a camel hairbrush on preheated samples (250 °C). Each sample was placed in the crucible and the weight was measured including the container and difference in weight had been noted. The Al_2O_3 container used for the studies were preheated at a constant temperature of 1200 °C for 18 h and it was assumed that their weight would remain constant during the course of high-temperature cyclic corrosion study. Weight-change measurements were taken at the end of each cycle using an electronic balance with a sensitivity of 1 mg. At the time of weighing, even the spalled scale was included to determine the total rate of corrosion. Efforts were made to formulate the corrosion kinetics. The surfaces of the corroded specimens were visually observed to record color, spalling, and peeling of the scale during cyclic corrosion. After corrosion testing, the samples were examined by SEM, EDAX, and XRD for surface analysis. The hot corroded samples were then cut across the cross section with a slow speed cutter (ISOMET 1000 Precision Diamond Cutter). These cross sections were then mounted, mirror polished and carbon coated to study the scale thickness and to perform x-ray mapping and EDAX analysis. EDAX analysis is done at Indian Institute of Technology, Kharagpur (India) on JEOL (JSM-5800) SEM fitted with EDAX attachment of the Oxford (Model-6841) made in England. The equipment could directly indicate the elements or phases (oxides) present at a point along with their compositions (wt%) based on built-in EDAX software, which is a patented product of Oxford ISIS300.

3. Results

3.1 Corrosion Kinetics

The weight gain per unit area (mg/cm^2) during corrosion tests for the steel substrates and the coatings is plotted with respect to time and presented in Fig. 1. Among all the coatings, the WC-Co coating showed the highest-weight gain, which was about 60% of the value obtained for the uncoated steel. NiCr wire-coated steel shows the lowest-weight gain throughout the entire range up to 50 cycles and is nearly 17 times lower than the one obtained for the uncoated steel in the given molten salt environment. The second lowest weight gain is indicated by the Cr_3C_2-NiCr, which is nine times lower than the uncoated steel. The uncoated and coated steels show a parabolic behavior. The uncoated steel has shown spalling right from the second cycle and peeling of the scale started from the fifth cycle. Also some small cracks were observed on the surface of the scale. The spalling of the scale for NiCr

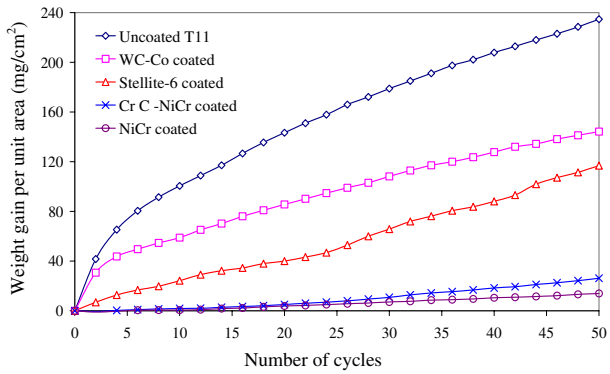

Fig. 1 Weight gain as a function of the number of cycles for coated and uncoated steels subjected to cyclic oxidation for 50 cycles in Na_2SO_4-60% V_2O_5 at 900 °C

and Cr_3C_2-NiCr coatings was minor and in the form of a greenish powder. The other two types of coatings indicated more spalling of the scale relative to NiCr and Cr_3C_2-NiCr coatings. Some embossing lines of gray colors were observed on the surface of the Cr_3C_2-NiCr coating right from the 19th cycle. The scale color formed onto the WC-Co and Stellite-6 coatings were blackish gray along with some cracks. The porosity levels of each coating are given in Table 4.

Table 4 Porosity levels of each coating (Ref 6)

Coating	Porosity, %
Cr_3C_2-NiCr	2.5-3.5
WC-Co	1.5-2.5
Stellite-6	2-3
NiCr (Wire)	>1

3.2 X-Ray Diffractometry Analysis

The x-ray diffractometry analysis has shown the formation of Fe_2O_3 as the main scale constituent along with Cr_2O_3 for the uncoated steel (Fig. 2). The NiCr and Cr_3C_2-NiCr coated steels have shown the presence of Fe_2O_3, Cr_2O_3, NiO, and $NiCr_2O_4$ phases in the scales. For the Stellite-6 coated steel, four more phases, $NiWO_4$, Fe_3O_4, $CoCr_2O_4$, and CoO are identified along with Fe_2O_3, Cr_2O_3, NiO, and $NiCr_2O_4$ phases. The scale of the WC-Co coated steel shows the phase like Fe_2O_3, Fe_3O_4, and CoO.

3.3 Scanning Electron Microscopy/Energy-Dispersive X-ray Analysis

3.3.1 Surface Morphology of the Scales. The SEM/EDAX micrographs showing the surface morphology of the specimens after cyclic hot corrosion are presented in

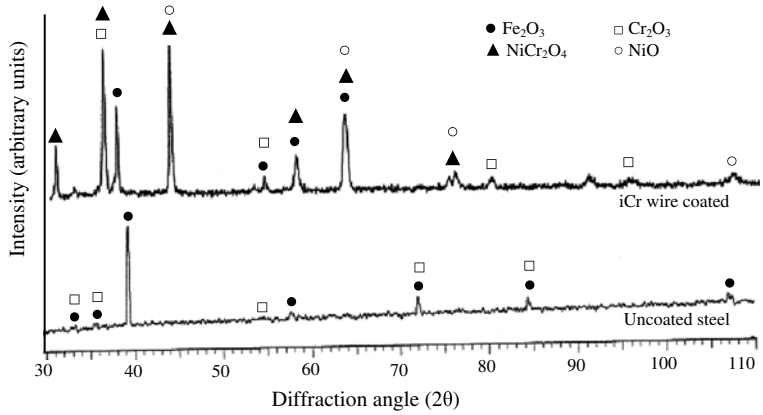

Fig. 2 X-ray diffraction spectra for steels exposed to cyclic oxidation for 50 cycles in Na_2SO_4-60% V_2O_5 at 900 °C

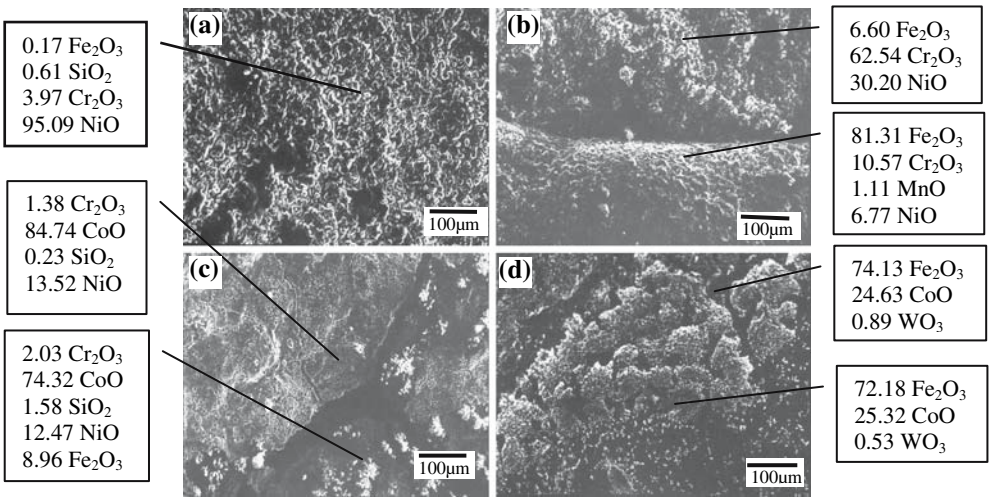

Fig. 3 Surface morphology and EDAX analysis after cyclic oxidation in Na_2SO_4-60% V_2O_5 at 900 °C for: (a) NiCr wire coated, (b) Cr_3C_2-NiCr coated, (c) Stellite-6 coated, and (d) WC-Co coated

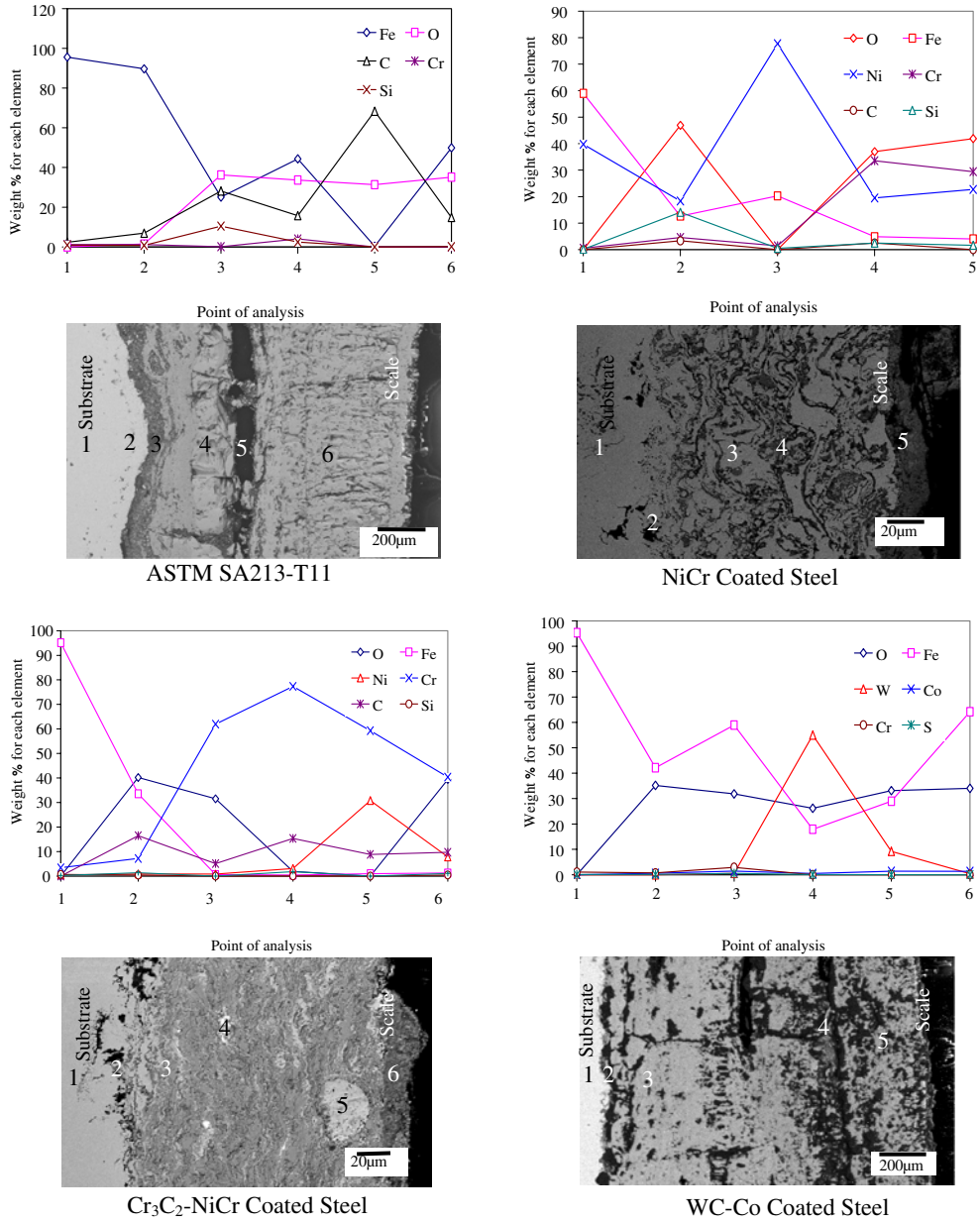

Fig. 4 Morphology and elemental variation along the cross sections of the oxide scale after cyclic oxidation in Na_2SO_4-60% V_2O_5 at 900 °C

Fig. 3. The EDAX analysis for the uncoated steel shows Fe_2O_3 to be the predominant phase. The EDAX analysis for the scale of the NiCr coated specimen indicated that the top surface consists mainly of NiO (95%). The scale of the Cr_3C_2-NiCr coated sample has higher-percentage of Cr_2O_3 and NiO along with other minor phases of Fe_2O_3 and MnO. The top surface of the Cr_3C_2-NiCr coated steel scale shows embossed lines, which are rich in Fe_2O_3 (81%). The scale of the Satellite-6 coated steel shows the dominance of CoO along with NiO, Fe_2O_3, and Cr_2O_3.

3.3.2 Cross-Sectional Analysis of the Oxide Scales. The formation of iron oxide, along the crosssection of the uncoated corroded steel sample was revealed by EDAX analysis as shown in Fig. 4. For the NiCr coated steel, high-amounts of Ni and Cr were revealed by EDAX analysis at point 4, and high amount of Ni also indicated by the point 3. Diffusion of iron and silicon from the substrate to the coating was also noticed. Accumulation of oxygen pockets was found at the coating substrate interface. High amount of Cr at points 3, 4, 5, and 6 was revealed by the EDAX analysis for the Cr_3C_2-NiCr coated steel. From the EDAX analysis of the scale formed on the WC-Co coated steel, oxygen seems to have penetrated into the substrate. The EDAX analysis of the WC-Co coated steel scale, along the cross section, has shown Fe_2O_3 and CoO as the predominant phases along with very small quantity of WO_3.

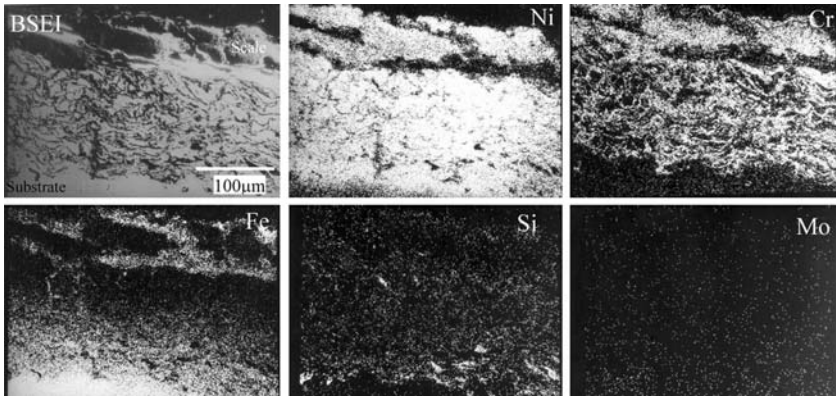

Fig. 5 Composition image (BSEI) and x-ray mapping of the cross section of the NiCr coated steel subjected to cyclic corrosion in molten salt at 900 °C

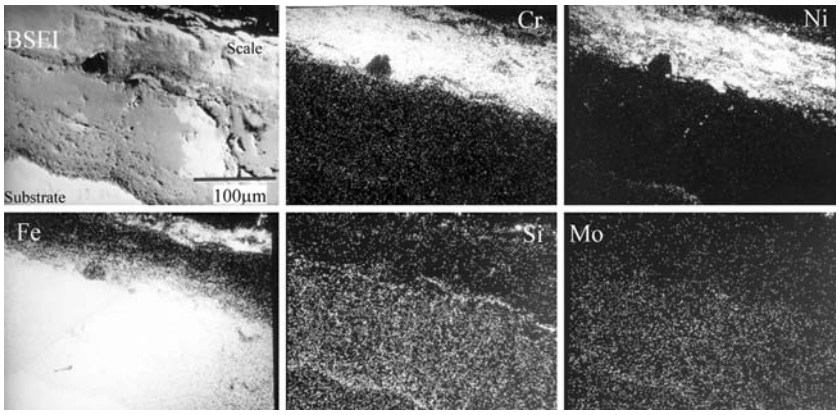

Fig. 6 Composition image (BSEI) and x-ray mapping of the cross section of the Cr_3C_2-NiCr coated steel subjected to cyclic corrosion in molten salt at 900 °C

3.4 Electron Probe Microanalysis

Electron probe microanalysis of the corroded cross-section of the uncoated ASTM SA213-T11 steel indicated the formation of Fe_2O_3. EPMA maps of the NiCr coated and corroded steel are presented in Fig. 5. From the first look on the BSE images, it immediately appears that the coating has retained its structure. Ni and Cr are present through out the scale. Fe has diffused from the substrate into the scale and has reached the top of scale, where a continuous layer of Fe is present. Si pockets in higher concentration are also present in the scale. Ni has also diffused into the substrate.

The EPMA mapping of the Cr_3C_2-NiCr coated steel (Fig. 6), indicated the formation of a Ni-rich and Cr-rich continuous layer in the top region of the scale. From the first look on the BSE images, it is clear that Fe has diffused from the substrate into the coating. Si is present in the scale in higher concentrations in the form of streaks. Mo is also present in a scattered manner.

EPMA mapping of the scale formed on the Satellite-6 coated steel shows Co rich layer at the top of the scale that also contains chromium. Si also precipitated to the substrate boundary. In all the coatings Fe has diffused from the substrate into the coating.

4. Discussion

The identification of Fe_2O_3 in the scales of the uncoated steel after hot corrosion experiments indicated that nonprotective conditions were established when Na_2SO_4-60% V_2O_5 molten salt was present on the surface. The formation of Fe_2O_3 in the spalled scale has also been reported (Ref 7) to be nonprotective during hot-corrosion study on iron aluminide alloys in Na_2SO_4 atmosphere. Intense spalling and peeling of the scale for this uncoated steel may be attributed to the Mo oxides, which cause an alloy-induced acidic flux (Ref 8). The higher corrosion rate during the initial hours of the study might be attributed to the rapid oxygen pick up by diffusion of oxygen through the molten salt layer and is identical to the results reported elsewhere (Ref 9, 10). These coatings also provided a good protection to the ASTM SA210 GrA1 steel when tested in the same environments at 900 °C (Ref 11).

The NiCr coating provided the best protection to the substrate steel, which may be due to the formation of NiO, $NiCr_2O_4$and Cr_2O_3 as confirmed by XRD, EPMA and EDAX analysis. These phases are reported to be protective oxides (Ref 10, 12). Hot corrosion resistance of the Cr_3C_2-NiCr coating is less as compared to the NiCr coating, however, its performance is better than the Stellite-6 and WC-Co coatings. For this corroded steel, the XRD, EPMA and EDAX analysis also confirm the formation of phases similar to the NiCr coated steel. However, comparatively higher-porosity values have lead to higher-corrosion rate for this coated steel. The protection behavior of coatings may be explained in view of the results reported by Uusitato et al. (Ref 13), where the corroding species were reported to propagate through the voids and to form an oxide at the splat boundaries of the coatings. Due to strongly flattened splats, the distance from the coating surface to the coating/substrate interface along the splat boundary is very long, and thus a high-corrosion resistance is offered by the coating. The protection shown by the Stellite-6 coating may be due to the formation of cobalt oxide, and spinals of chromium and cobalt. EDAX analysis shows a higher percentage of cobalt at the surface of the scale. The WC-Co coating shows the least resistance to hot corrosion, which is believed to be due to the formation of a nonprotective Fe_2O_3.

5. Conclusion

The NiCr, Cr_3C_2-NiCr, WC-Co, and Stellite-6 coatings can be successfully applied to the boiler tube steel by the HVOF spray process using LPG as the fuel gas. Fe_2O_3 was identified as the major phase by XRD, EDAX, and EPMA analysis in the scale of the uncoated steel. The NiCr coating shows the lowest value of porosity and provides the highest resistance to hot corrosion. Formation of protective oxides like Cr_2O_3, NiO and $NiCr_2O_4$ in the scale may contribute to the better corrosion resistance of coatings. Minimum protection has been provided to the substrate steel by the WC-Co coating, in which peeling-off, spalling and cracking of the coating was observed.

References

1 R.A. Rapp, Chemistry and Electrochemistry of the Hot Corrosion of Metals, *Corrosion*, 1986, **42**(10), p 568-577
2 D. Wang, Corrosion Behavior of Chromized and/or Aluminized 2.25Cr-1Mo Steel in Medium-BTU Coal Gasifier Environments, *Surf. Coat. Technol.*, 1988, **36**, p 49-60
3 P.S. Sidky and M.G. Hocking, Review of Inorganic Coatings and Coating Processes For Reducing Wear and Corrosion, *Brit. Corros. J.*, 1999, **34**(3), p 171-183
4 B.S. Sidhu and S. Parkash, Degradation Behavior of Ni_3AL Plasma-Sprayed Boiler Tube Steels in an Energy Generation System, *J. Mat. Eng. Perform.*, 2005, **14**(3), p 356-362
5 J. Stokes and L. Looney, Residual stress in HVOF thermally sprayed thick deposits, *Surf. Coat. Technol.*, 2004, **177-178**, p 18-23
6 H.S. Sidhu, B.S. Sidhu, and S. Prakash, Mechanical and Microstructural Properties of HVOF sprayed WC-Co and Cr_3C_2-NiCr Coatings on the Boiler Tube Steels Using LPG as the Fuel Gas, *J. Mat. Process. Technol.*, 2006, **171**, p 77-82
7 D. Das, R. Balasubramaniam, and M.N. Mungole, Hot Corrosion of Fe_3Al, *J. Mater. Sci.*, 2002, **37**(6), p 1135-1142
8 F.S. Pettit and C.S. Giggins, Hot Corrosion, Chap. 12, *Superalloys II*, C.T. Sims, N.S. Stollof, and W.C. Hagel, Eds., Wiley, NY, 1987
9 B.S. Sidhu and S. Parkash, Evaluation of the Corrosion Behaviour of Plasma-Sprayed Ni_3Al Coatings on Steel in Oxidation and Molten Salt Environment at 900°C, *Surf. Coat. Technol.*, 2003, **166**(1), p 89-100
10 A. Ul-Hamid, Diverse Scaling Behavior of the Ni-20Cr Alloy, *Mater. Chem. Phys.*, 2003, **80**, p 135-142
11 H.S. Sidhu, B.S. Sidhu, and S. Prakash, The Role of HVOF Coatings in Improving Hot Corrosion Resistance of ASTM-SA210 GrA1 Steel in the Presence of Na_2SO_4-V_2O_5 Salt Deposits, *Surf. Coat. Technol.*, 2006, **200**, p 5386-5394
12 T. Sundararajan, S. Kuroda, T. Itagaki, and F. Abe, Steam Oxidation Resistance of Ni-Cr Thermal Spray Coatings on 9Cr-1Mo Steel. Part 2: 50Ni-50Cr, *ISIJ Int.*, 2003, **43**(1), p 104-111
13 M.A. Uusitalo, P.M.J. Vuoristo, and T.A. Mantyla, High Temperature Corrosion of Coatings and Boiler Steels in Reducing Chlorine-Containing Atmosphere, *Surf. Coat. Technol.*, 2002, **161**, p 275-285